3.10.2.4. *Variable amorphous content series*

A constant matrix of calcite (C) and zincite (Z) was prepared. Five samples with increasing contents of amorphous ground glass (Gl) were then prepared. The elemental composition of the ground glass is given in García-Maté *et al.* (2014). The mixtures were labelled CZQ_*x*Gl, where *x* indicates 0, 2, 4, 8, 16 or 32 wt% Gl. The amorphous content was determined by adding ∼20 wt% quartz (Q) as an internal standard.

3.10.3. Analytical techniques

All phases and mixtures were studied with Mo $K\alpha_1$ (transmission geometry) and Cu $K\alpha_1$ (reflection geometry) monochromatic radiation. Table 3.10.1 shows the X-ray linear absorption coefficients for all of the phases, as microabsorption is always a concern in RQPA. A microabsorption correction was not applied in this work, but readers must be aware that this effect, if relevant, is one of the greatest source of inaccuracy in RQPA (Madsen *et al.*, 2001; Scarlett *et al.*, 2002). All of the phases were also characterized by scanning electron microscopy (see Fig. 3.10.2).

3.10.3.1. *Mo $K\alpha_1$ laboratory X-ray powder diffraction (LXRPD)*

Mo $K\alpha_1$ powder patterns were collected in transmission geometry in constant irradiated volume mode, in order to avoid any correction of the measured intensities, on a D8 ADVANCE (Bruker AXS) diffractometer (188.5 mm radius) equipped with a Ge(111) primary monochromator, which gives monochromatic Mo radiation (λ = 0.7093 Å). The X-ray tube operated at 50 kV and 50 mA. The optics configuration was a fixed divergence slit (2°) and a fixed diffracted anti-scatter slit (9°). A LYNXEYE XE 500 µm energy-dispersive linear detector, optimized for high-energy radiation, was used with the maximum opening angle. Using these conditions, the samples were measured between 3 and 35° 2θ with a step size of 0.006° and with a total measurement time of 3 h 5 min. The flat samples were placed into cylindrical holders between two Kapton foils (Cuesta *et al.*, 2015) and rotated at a rate of 10 revolutions per minute during data collection. Moreover, the absorption factor of each sample was experimentally measured by comparing the direct beam with and without the sample (Cuesta *et al.*, 2015). The amount of sample loaded (which determines the height of the cylinder) in the holders was adjusted to obtain a total absorption (μt) of ∼1, which corresponds to an absorption factor of ∼2.7 or 63% of direct-beam attenuation. For the organic samples this criterion was not followed as it would lead to very thick specimens. In this case, the maximum holder thickness was used (1.7 mm).

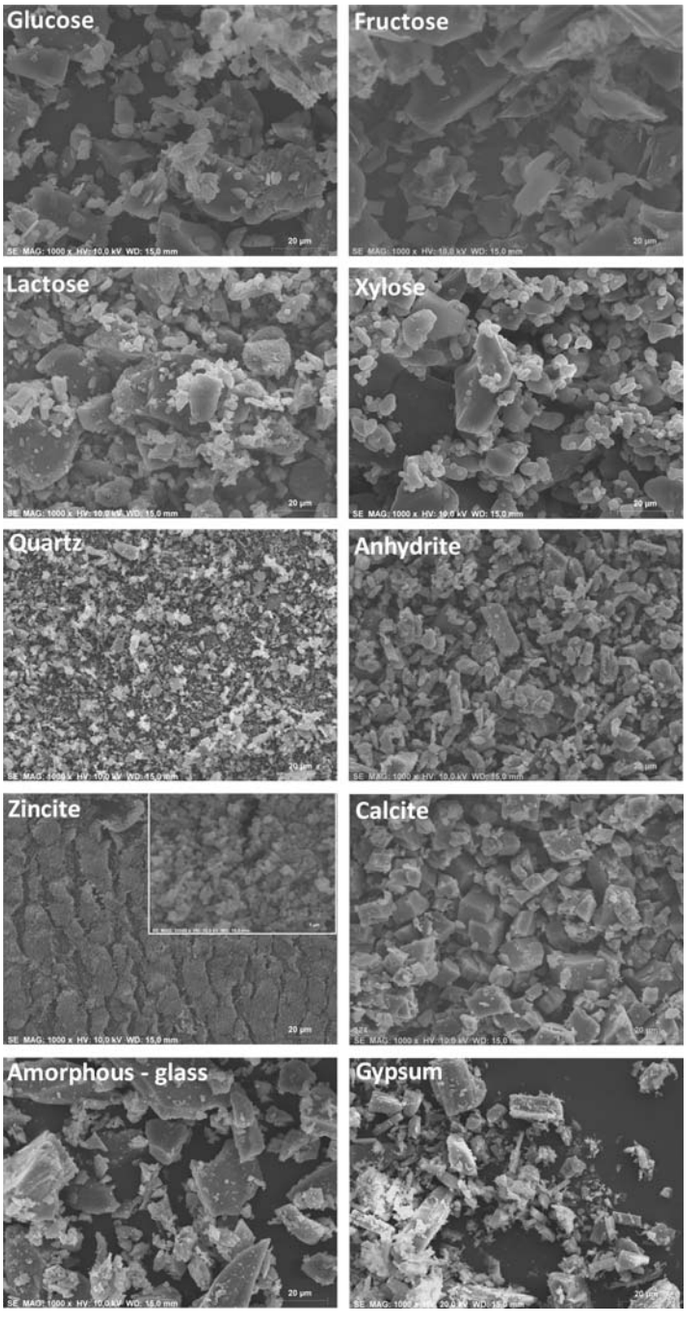

Figure 3.10.2
Scanning electron microscopy micrographs for the studied phases (×1000). The inset in the zincite micrograph shows the powder at higher magnification (×20 000).

3.10.3.2. *Cu $K\alpha_1$ laboratory X-ray powder diffraction (LXRPD)*

Cu $K\alpha_1$ powder patterns for exactly the same samples were recorded in reflection geometry ($\theta/2\theta$) on a X′Pert MPD PRO (PANalytical B.V.) diffractometer (240 mm radius) equipped with a Ge(111) primary monochromator, which gives monochromatic Cu radiation (λ = 1.54059 Å). The X-ray tube was operated at 45 kV and 40 mA. The optics configuration was a fixed divergence slit (0.5°), a fixed incident anti-scatter slit (1°), a fixed diffracted anti-scatter slit (0.5°) and an X′Celerator RTMS (real-time multiple strip) detector operating in scanning mode with the maximum active length. Using these conditions, the samples were measured between 6.5 and 81.5° 2θ with a step size of 0.0167° and a total measurement time of 2 h 36 min. The flat samples were prepared by rear charge of a flat sample holder in order to minimize preferred orientation and were rotated at a rate of 10 revolutions per minute.

The lowest analyte content samples, CGpQ_0.12A and GFL_0.12X, were measured three times using both radiations, Mo $K\alpha_1$ and Cu $K\alpha_1$, for a precision (reproducibility) assessment. Therefore, regrinding and reloading of the mixtures in the sample holder was carried out prior to every measurement.

3.10.3.3. *Transmission synchrotron X-ray powder diffraction (SXRPD)*

Powder patterns for the lowest analyte content samples, CGpQ_0.12A and GFL_0.12X, were also measured using synchrotron radiation. SXRPD data were collected in Debye–Scherrer (transmission) mode using the powder diffractometer at

the ALBA Light Source (Fauth *et al.*, 2013). The wavelength, λ = 0.77439 (2) Å, was selected with a double-crystal Si(111) monochromator and was determined using the NIST SRM640d Si standard (a = 5.43123 Å). The diffractometer is equipped with a MYTHEN-II detector system. The samples were loaded into glass capillaries 0.7 mm in diameter and were rapidly rotated during data collection to improve the diffracting-particle statistics. The data-acquisition time was 20 min per pattern to attain a very good signal-to-noise (S/N) ratio over the angular range 1–35° 2θ. Three patterns, taken at different positions along the capillaries, were collected for each sample.

SXRPD data for the amorphous content series, CZQ_xGl, were also measured at the ALBA Light Source. The experimental setup was the same as described above but the working wavelength was λ = 0.49591 (2) Å.

3.10.4. Powder-diffraction data analysis

All powder patterns were analysed by the Rietveld method using the *GSAS* software package (Larson & Von Dreele, 2000) with the pseudo-Voigt peak-shape function (Thompson *et al.*, 1987) for RQPA. The refined overall parameters were phase scale factors, background coefficients (linear interpolation function), unit-cell parameters, zero-shift error, peak-shape parameters and preferred-orientation coefficient, when needed. The March–Dollase preferred-orientation adjustment algorithm was employed (Dollase, 1986). The modelling direction must be given as input for the calculations. In this case, the directions for the different phases were taken from previous studies. Alternatively, this direction can be extracted from the pattern from an analysis of the differences between observed and calculated intensities for non-overlapped diffraction peaks. The crystal structures used are reported in Table 3.10.1.

In order to provide a single numerical assessment of the performance of each analysis, a statistic based on the KLD distance was used (Kullback, 1968). This approach was previously used to evaluate the accuracy of RQPA applied to standard mixtures (Madsen *et al.*, 2001; Scarlett *et al.*, 2002; León-Reina *et al.*, 2009). Both phase-related KLD distances and absolute values of the Kullback–Leibler distance (AKLD) were calculated. Accurate analyses are mirrored by low values of AKLD.

The overall amorphous content was determined from the internal standard methodology approach (De la Torre *et al.*, 2001; Aranda *et al.*, 2012) with quartz as an internal standard [using isotropic atomic displacement parameters (ADPs) of 0.045 and 0.0087 Å^2 for Si and O, respectively]. If the original sample contains an amorphous phase, the amount of standard will be overestimated in RQPA. From the (slight) overestimation of the standard, the amorphous content of the investigated sample can be derived (De la Torre *et al.*, 2001). The important role of the values of the ADPs in the results of RQPA mainly in amorphous content determinations using the internal-standard method has been discussed previously (Madsen *et al.*, 2011).

3.10.5. Crystalline single phases

All of the single phases were selected according to several parameters, such as relevance to selected applications, purity, particle size of the powder and preferred orientation. In order to check the suitability of the crystal structures used, all of the phases were first studied using powder diffraction with Mo $K\alpha_1$ radiation. These preliminary studies were of special interest for organic phases, as the CIF files obtained from the Cambridge Structural Database (CSD) did not contain the atomic displacement parameters (ADPs). For lactose and fructose, the ADPs were obtained from the original publications and were introduced manually into the *GSAS* control file. For glucose and

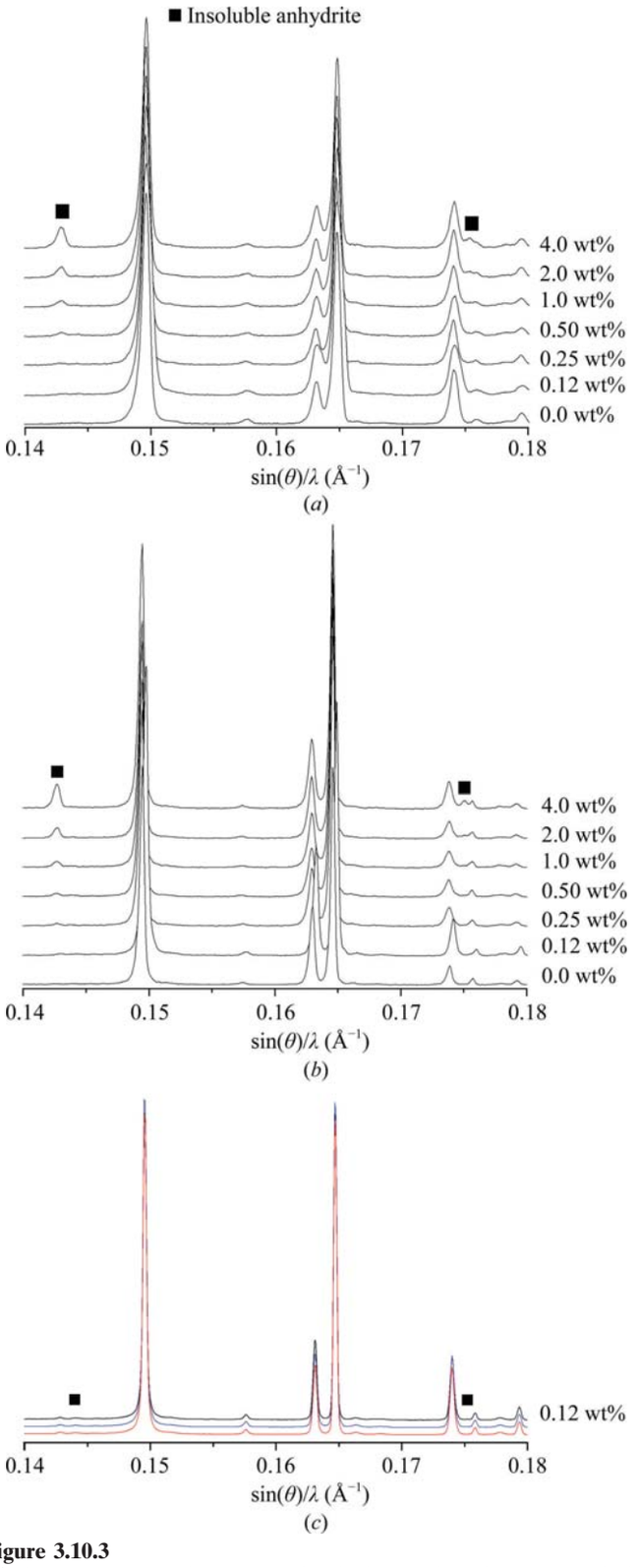

Figure 3.10.3
(*a*) Raw Mo $K\alpha_1$ powder patterns for the inorganic series composed of a constant matrix of calcite, gypsum and quartz, and increasing amounts of insoluble anhydrite (peaks highlighted with a solid square). (*b*) Raw Cu $K\alpha_1$ powder patterns for the same inorganic series. (*c*) Raw SXRPD patterns for CGpQ_0.12A collected at three different positions of the capillary (red, black and blue traces). The intensity values in (*c*) have been artificially offset to show the three different patterns.

references